Rapid Compression of Aluminum Alloys and Its Relationship to Thixoformability

T.Y. LIU, H.V. ATKINSON, P. KAPRANOS, D.H. KIRKWOOD, and S.C. HOGG

Shaping of metals by thixoforming relies on the unusual flow behavior of semisolid slurries containing nondendritic solid phase. The microstructure of an alloy stirred during freezing consists of rounded particles of solid, as opposed to the dendrites associated with conventional solidification. In the semisolid state, these slurries are thixotropic, in that their apparent viscosity is dependent on shear rate and time. Here, a technique of rapid compression testing is outlined, carried out under conditions similar to normal industrial thixoforming, to assess slurry flow behavior and to examine the correlation between feedstock production routes, microstructure, and resistance to flow. Samples are heated to the desired temperature in the semisolid state with various soaking times and rammed at constant velocity against a platen backed by a load cell. The load-displacement curves produced from the tests may show an initial peak, believed to originate from a skeletal structure which rapidly breaks down under shear. The load signal during flow decreases with increasing soaking time and with temperature, and the initial peak eventually disappears in all alloys investigated. Quantitative metallography indicates that the lower loads correspond to greater spheroidicity of the solid particles within the slurry. The curves have been analyzed to derive the viscosity as a function of average shear rate and demonstrate that the semisolid slurries exhibit pseudoplastic flow behavior which is dependent on the compression velocity and is far removed from steady-state conditions.

I. INTRODUCTION

SEMISOLID processing is a novel method of forming complex-shaped components in the semisolid state. This near-net-shape method was first introduced in the 1970s, and the key to this process is the internal nondendritic microstructure, which gives the alloys thixotropic properties in the semisolid state.[1,2] Originally, researchers obtained alloys with a nondendritic microstructure by cooling a fully liquid alloy to its semisolid state while applying vigorous agitation by mechanical stirring throughout solidification. Upon reaching the desired solid fraction, the semisolid alloy slurry was then injected into a shaped die (in a process also known as Rheocasting[3]). Mechanical testing of rheocast components showed that they possessed better properties than those produced by liquid casting.[3] Furthermore, shaping in the semisolid state meant that the work required to generate a component is less than that for solid forging.[3,4] The vigorous agitation of metal alloys during solidification leads to the formation of spheroidal solid particles suspended in the liquid matrix through a process of dendrite-arm detachment and coarsening. Such semisolid microstructures exhibit thixotropic behavior (*i.e.*, a decrease in viscosity during shearing, followed by gradual recovery with time when shearing is halted). When fully solidified and then reheated to the semisolid state again, they can be cut and spread like butter, but thicken again when allowed to stand. This phenomenon is largely due to the breakup of the agglomerate structure of solid particles during an increase in the shear rate. Once a shear-rate change (to a higher shear rate) has taken place, the agglomerate size will then decrease over time to an equilibrium size appropriate to the higher shear rate. The higher the shear rate, the more the agglomerates disintegrate, eventually consisting of just the constituent primary particles that tend to slide past each other, with the liquid matrix acting as a lubricant. If the shear rate is now changed from a high value to a low value, collisions and agglomeration will occur as a result of the reduced movement in the slurry, until, with time, the size of the new agglomerate structure is the equilibrium value appropriate to the lower shear rate.

The mechanical-stirring route of producing feedstock for semisolid processing has a number of drawbacks, the most obvious being that it is only suitable for "batch," rather than continuous, production. In order to enhance the commercial potential of processing alloys in the semisolid state, other more suitable methods of producing the necessary semisolid alloy feedstock have been tried over the years.[5–10] Instead of mechanical stirring, a magnetohydrodynamic (MHD) stirring process has been developed.[5,6] In this technique, liquid melt passes through a rotating electromagnetic field within a continuous-casting mold. The resulting alloy billets have more spheroidal and equiaxed microstructures as opposed to the highly elongated dendritic microstructure typical of conventional cast alloys. This process has a number of advantages over the mechanically stirred alloys, in that there is little contamination by oxidation during the forming of the thixotropic feedstock and that much finer and more uniform grains are obtained in the microstructure. In addition, this route is suitable for continuous casting of large quantities of feedstock, appropriate to commercial industrial applications. The feasibility of producing semisolid alloy feedstock by solid-state routes has also been demonstrated. Two such methods are

T.Y. LIU, formerly a PhD Student with the Department of Engineering Materials, University of Sheffield, Sheffield, UK S1 3JD, can now be contacted at Blk 418, #10-304, Choa Chu Kung Ave 4, Singapore 680418. H.V. ATKINSON, formerly Reader with the Department of Engineering Materials, University of Sheffield, S1 3JD UK, is now Professor, Department of Engineering, University of Leicester, LEI 7R11, UK. Contact e-mail: hva2@le.ac.uk P. KAPRANOS, Senior Research Fellow, and D.H. KIRKWOOD, Honorary Senior Lecturer, are with the Department of Engineering Materials, University of Sheffield, Sheffield, S1 3JD UK. S.C. HOGG, formerly Research Fellow with the Department of Engineering Materials, University of Sheffield, S1 3JD, UK, is Research Fellow with the Sprayforming Research Group, Department of Materials, University of Oxford, Oxford, OXS 1PF UK.

Manuscript submitted July 15, 2002.

the strain-induced, melt-activated (SIMA) and recrystallization and partial melting (RAP) processes.[7,8] Both processes make use of a deformation-plus-recrystallization route. The microstructure of a material that is sufficiently deformed will change upon partial remelting from an elongated one (along the direction of the deformation) to one consisting of rounded spheroidal particles in the liquid matrix. In the SIMA process, deformation of the alloys is primarily carried out above the recrystallization temperature (*i.e.*, hot working), while the RAP process takes place below the recrystallization temperature (*i.e.*, warm working). Another approach used for producing a spheroidal structure in the feedstock involves heating a dendritic structure to the semisolid temperature range for a period of time sufficient to allow a spherical structure to evolve. This is known as semisolid thermal transformation, or SSTT.[9]

Other feedstock production processes include sprayforming (Osprey process),[10] the shear-cooling roll (SCR) process,[11] the cooling slope process,[12] and the New Rheocasting (NRC) process[13] patented by UBE Industries Ltd. In NRC, conventional cast material can be used, opening the way for recycling. Hall *et al.*[14] carried out a cost analysis of the NRC route and showed that it has a lower per-unit cost (~20 pct lower) compared to conventional thixoforming using MHD feedstock, due to the lower starting-material cost. However, this method has certain disadvantages: namely, the material is more fluid during the forming process, encouraging turbulent flow during filling and gas entrapment.

In order to produce complex near-net-shape parts by semisolid processing, two different approaches have been employed (Figure 1). Thixocasting is where the feedstock is forced into a die cavity as in a die-casting machine, and thixoforging is where the feedstock is forged between two dies. The work at the University of Sheffield currently employs a vertical computer-controlled hydraulic thixoforming press (Figure 2),[15] where the feedstock or billet is heated to its semisolid state by *in-situ* induction heating and forced upward into either heated or cold closed dies. The work described in this article expands on the work carried out previously,[16,17,18] examining material from a greater variety of feedstock routes, investigating the effect of variations in compression speed, and analyzing the shear-thinning exponent (derived from a power-law model) for various feedstock alloys. The test involves the rapid compression of cylindrical slugs in the semisolid state on the thixoforming press into a die incorporating a load cell. The load *vs* displacement-response curve can be correlated with the microstructure, and this provides a novel way of assessing the thixoformability of alloy feedstock and the breakdown behavior.

Previous work carried out by Laxmanan and Flemings[19] on Sn15 pct Pb alloys measured the force and displacement for this low-temperature alloy by slow compression. However, in the experiments carried out, the resulting load was not measured directly (but, rather, derived from the pressure on the ram), and the rate of compression was much slower than in the industrial process, where die filling takes place in less than 1 second. The industrial process also uses higher-temperature alloys (*viz.*, aluminum alloys). The work of Loué *et al.*,[20] carried out at higher shear rates by backward extrusion on aluminum alloys, resembles more closely industrial thixoforming. However, the specimens are heated to temperature over long period of time (~10 minutes) and then held isothermally for 30 minutes before compression. Such time periods are considered long in industrial thixoforming. The work here investigates aluminum feedstock alloys used in thixoforming. The testing takes place at high compression rates, more akin to industrial thixoforming, and the load is measured directly from a load cell placed on top of the die. The whole process (from heating to compression) takes place in less than 10 minutes.

II. EXPERIMENTAL PROCEDURES

The rapid-compression experiments are carried out on the vertical thixoforming press (Figure 2). Heating is controlled by an induction heating system that allows accurate control of the temperature to within 1 °C in the slugs. The frequency can be varied from 800 Hz to 10 kHz, with a maximum power of 100 kW. The rapid-compression experiments allow investigations of both higher-temperature alloys and higher-fraction solids than can be achieved by using a rotating viscometer. The cylindrical specimen or slug (dimensions: 42-mm high and diameter of 36 mm) is placed on a ceramic pedestal and heated to its desired temperature (or fraction

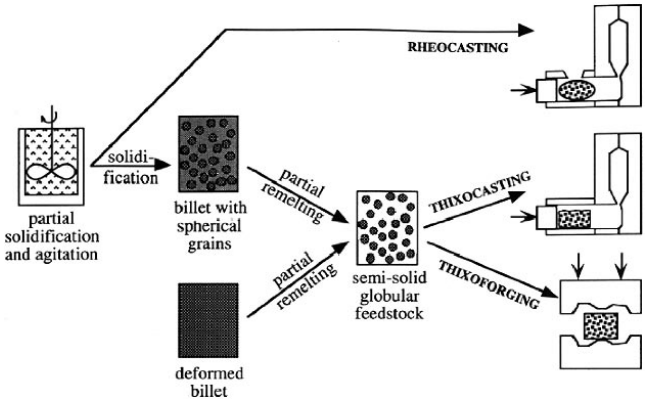

Fig. 1—Schematic illustration of different routes for semisolid metal processing.

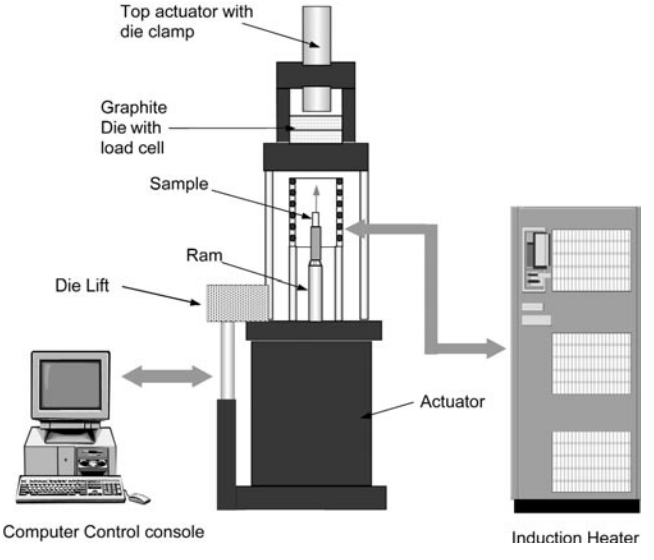

Fig. 2—Schematic diagram of the vertical thixoforming press used at Sheffield University for the rapid compression experiments.

of solid (f_s)). Upon reaching the desired temperature, the slug can either be held at that temperature for a period of the soaking time (providing the material does not slump) or be forced immediately into a die, which can be heated or nonheated, metallic or nonmetallic. The ram speed used throughout was 500 mm/s, unless otherwise stated. In these experiments, a nonmetallic (graphite) circular nonheated die is used, where the slug after forging has dimensions of 10 mm in height and 72 mm in diameter (Figure 3). Temperature uniformity was checked by the use of two thermocouples, one at the edge and another placed in the center of the specimen. The compression load is recorded as a function of time onto a computer *via* the load cell located on top of the die (Figure 4). A full description of the load-cell arrangement and its sensitivity is given in Reference 18. The average shear rate can be estimated analytically, following the work of Dienes and Klemm[21] in solving Stefan's equation for flow between two parallel planes.

Table I shows the compositions of the aluminium alloys tested and their feedstock (raw material) production routes. The forging press is controlled by a computer equipped with a Servotest DCS 2000 digital control system. The data-collection acquisition rate can be up to 2 kHz. The software allows a number of parameters to be specified by the operator. They are the speed of transfer of the slug into the die, the velocity profile of the ram during the slug's injection into the die, the magnitude of the final load applied, and the time duration of its application (*i.e.*, final holding or dwell time). Analogue signals obtained from the load cell are collected by the computer controller and can be easily transferred into MICROSOFT WINDOWS EXCEL* software for analysis. Experiments were carried out under different conditions, as follows.

*MICROSOFT, WINDOWS, and EXCEL are trademarks of the Microsoft Corporation, Redmond, WA.

(1) Varying temperatures (hence, the fraction of solid). The specimens were heated to different temperatures before the compression experiments. The load signal is then related to the displacement of the pedestal. The fraction of solid is usually above 0.5 in the rapid-compression experiments.
(2) Varying the soaking time. Specimens were held for a range of times (0 to 5 minutes) at the specified temperature before compression. Care has to be taken to ensure that the specimen is able to continue to support its own weight without slumping prior to compression.
(3) Varying the ram speed (the injection speed at which the compression experiments are carried out). Several speeds were employed. They ranged from 250 to 1000 mm/s. In these experiments, both the temperature and soak time were held constant.

An image analyzer has been used to capture the microstructures of metallographically prepared specimens obtained from these compression experiments, and values of the particle areas and their perimeters were obtained. The spheroidicity

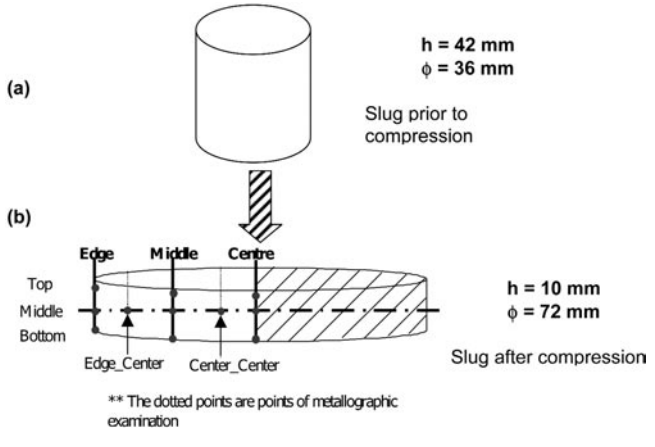

Fig. 3—Schematic diagram of slug (*a*) before rapid compression and (*b*) after rapid compression, and points of metallographic examination used in determining the form factors.

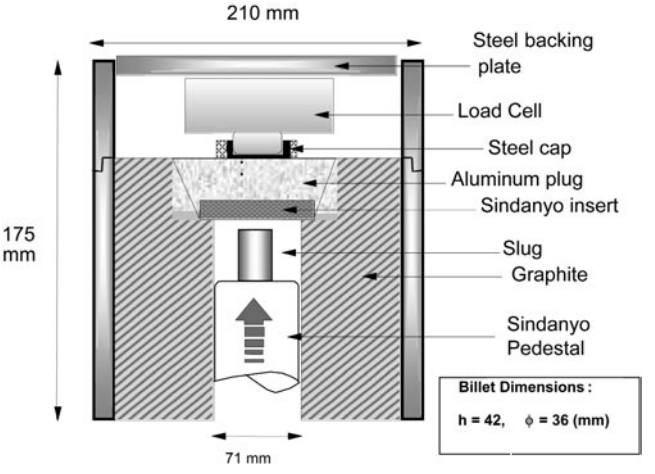

Fig. 4—Schematic diagram of the load cell used in the thixoforming machine to record the load *vs* time signals.

Table I. Compositions and Production Routes of Aluminum Alloys Tested in Rapid Compression Testing

Manufacturer	Alloy	Composition (Pct)*			Production Routes**
		Si	Cu	Mg	
Alusuisse	A356	6.6	0.03	0.35	MHD
North West Aluminum	A319	6.0	3.0	0.09	SSTT
North West Aluminum	A357	6.74	—	0.49	SSTT
Sheffield	A357	7.17	—	0.51	RAP

* *Chemical analysis of samples determined by inductively coupled plasma (atomic emission spectroscopy) technique.*
** *For descriptions of the various production routes, see Section I.*

of the particles is measured by employing the formula proposed by Witulski *et al.*:[22]

$$\text{Form factor (FF)} = \frac{4\pi(\text{Area})}{(\text{Perimeter})^2} \quad [1]$$

where a value of 1 indicates a completely spherical particle.

III. RESULTS

Figure 5(a) shows a typical load-signal response from the rapid-compression experiments. The graph shows load plotted against the displacement of the slug. The zero is given on the right-hand side, as this is the zeroing position for the ram, *i.e.*, its maximum height in the die where it touches the top plate. This position is used in the setting-up procedure, and all the data are recorded in relation to this zero. It will be noted that in the experimental curves, the load increases suddenly at around 44 mm rather than at the nominal height of the slug (of 42 mm). Uniform thermal expansion of the billet together with expansion due to partial melting will account for much of this difference. It is assumed that nonuniform expansion creating an irregular top surface must account for the remaining discrepancies. The slug height (h_0) used in later calculations is derived from the displacement of the ram from the load cell (*i.e.*, the initial "contact" point, Figure 5(a)). Errors in h_0 will lead to small errors in the viscosity calculations, especially at the initial stage of compression. It is estimated that a 1 mm error in h_0 will produce a 10 pct error in the calculated viscosity. A peak load (L_1) is encountered when the slug first touches the Sindanyo insert (Figure 4) in the die. This is followed by a drop in the load to a minimum value (L_2) during the rapid compression of the slug. As the material fills the die, the force recorded by the load cell increases during the final stages of compression. The repeatability in terms of peak height and minimum load is $\sim\pm 0.25$ kN (Figure 5(b)). Figures 6 through 8 show the effect of temperature on the Alusuisse A356, Northwest Al A319, and Sheffield A357 slugs under rapid compression (at 500 mm/s and zero soaking). The three graphs all show similar behavior, where the peak load decreases with increasing temperature. At the highest temperature used (Figure 6), it can be seen that the peak load has almost disappeared.

The equivalent microstructures of the alloys after rapid-compression experiments are shown together with their load-signal behavior in Figures 6 through 8. The microstructures show that with increasing temperature and, therefore, increasing fraction of liquid, the particles become more spherical in shape. This would account for the lower load signal encountered with increasing temperature, as the spherical particles move more freely than nonspherical particles. As the liquid fraction increases, there is a reduction in the number of interparticle contacts (necks) per particle. This reduces the viscosity. Figure 9 shows the effect of soaking

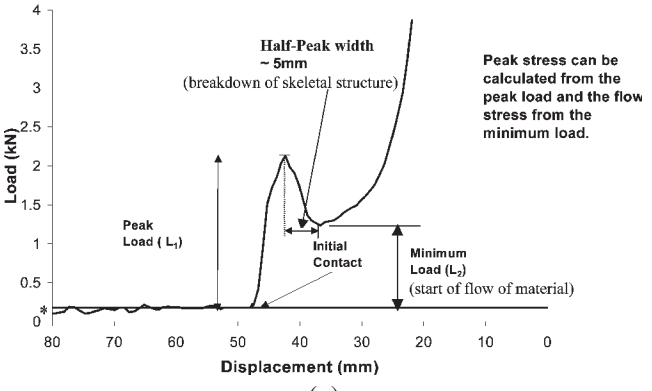

Fig. 5—(*a*) Typical signal response to rapid compression of a semisolid alloy slug. (*b*) Repeatability of thixoforming Alusuisse A356 alloys under similar conditions (ram speed: 500 mm/s; soak time: 0 minutes; and temperature: 575 °C). *The load signal is not initially at zero due to the clamping force on the die. This gives an offset signal. This offset can be seen throughout the whole process with the die clamped at all times.

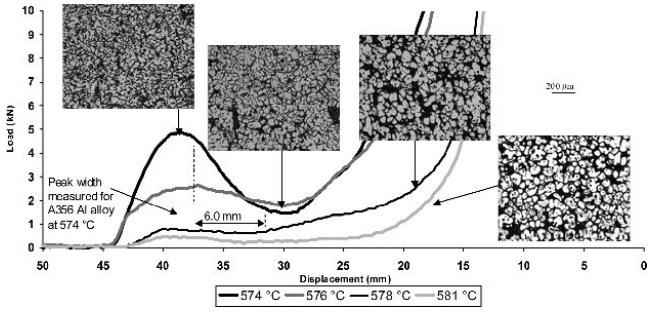

Fig. 6—Load signals and microstructures at different temperatures for Alusuisse A356 Al Alloy (ram speed: 500 mm/s, 0 soak). Microstructures are taken from Edge_Center (Fig. 3) of the slug after compression has been completed.

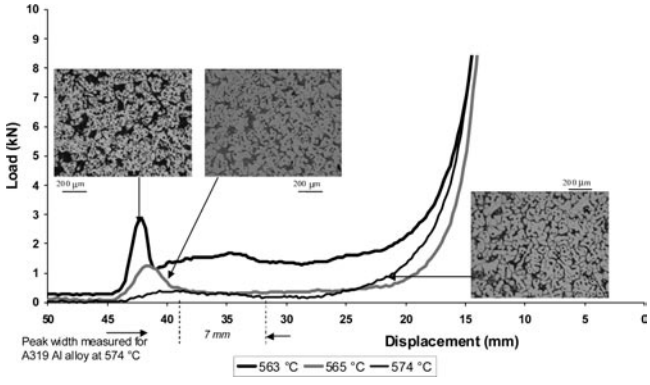

Fig. 7—Load signals and microstructures at different temperatures for NorthWest A319 Al alloy (ram speed: 500 mm/s, 0 soak). Microstructures are taken from the Edge_Center (Fig. 3) of the slug after compression has been completed.

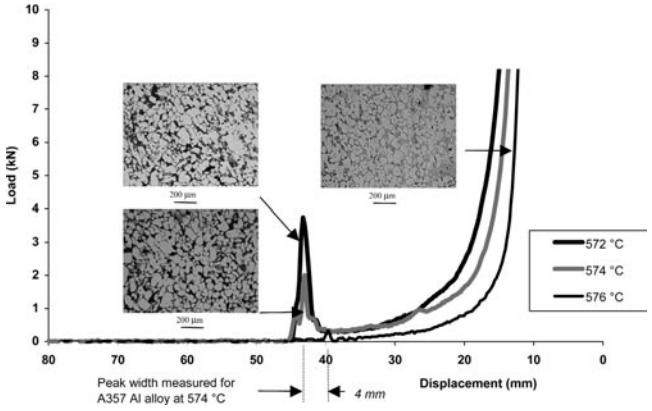

Fig. 8—Load signals and microstructures at different temperatures for Sheffield A357 Al alloy (ram speed: 500 mm/s, 0 soak). Microstructures are taken from the Edge_Center (Fig. 3) of the slug after compression has been completed.

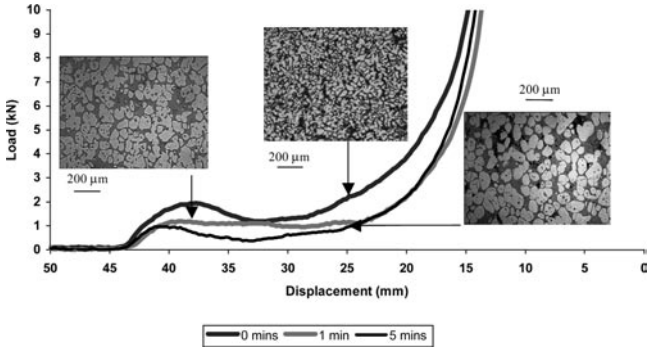

Fig. 9—Load signals and microstructures at different soaking times for Alusuisse A356 Al alloys at 575 °C (ram speed: 500 mm/s). Microstructures are taken from the Edge_Center (Fig. 3) of the slug after compression has been completed.

times on the load signals from rapid-compression experiments on Alusuisse A356 Al alloys (at 500 mm/s and $T = 575$ °C). With increasing holding times at the same temperature, the peak-load signal encountered during the experiments decreases. The microstructures, shown together with the graphs, indicate a similar behavior to that of the different temperature experiments. With increasing holding times, the particles became more spheroidal, resulting in the decrease in the load signal. Experiments were then conducted for the same alloy composition at a lower temperature under different soaking times (Figure 10). The peak load was observed to be higher than when the experiment was conducted at a higher temperature (Figure 9), but, more importantly, the peak load decreases with increasing soaking time.

Figure 11 shows the load-signal behavior at different ram speeds (with a constant temperature of $T = 576$ °C and constant (in this case, zero) soaking) for Alusuisse A356 Al alloys. Figure 11 shows that with decreasing ram speed, the peak-load signal decreases. The decrease in peak signal must be associated with a microstructural effect. At a lower ram speed, there is more time for the necks between particles to be broken during the initial thrust into the die, and, hence, the peak-load signal will be lower than that for higher ram velocities.

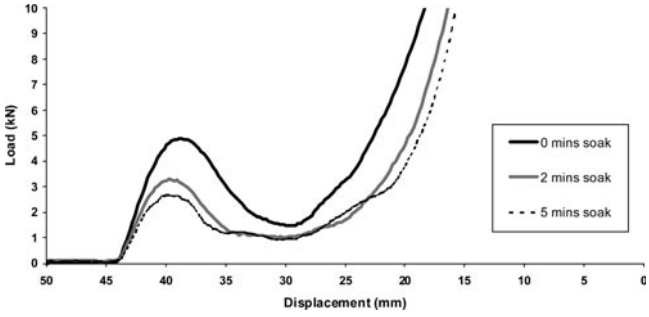

Fig. 10—Load signals and microstructures at different soak times for Alusuisse A356 Al alloys at 574 °C (ram speed: 500 mm/s).

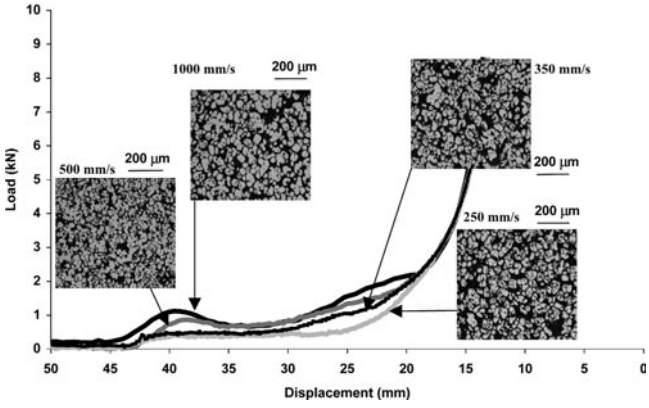

Fig. 11—Load signals and microstructures at different ram speeds for Alusuisse A356 Al alloys at 576 °C and 0 soak. Microstructures are taken from the Edge_Center (Fig. 3) of the slug after compression has been completed.

Table II. Calculated Form Factors of Various Thixoformed Alloys; Form Factors Measured on the Final Microstructure at Edge_Center of the Specimen (Figure 3); Ram Speed 500 mm/s; Where Temperature Is Being Varied, the Soaking Time Is Zero, Where Soaking Time Is Being Varied, the Temperature is 575 °C

Alusuisse A356 Alloys					
Temperature (°C)	574	576	578	579	
Form factor	0.63	0.64	0.66	0.67	
Soaking time (min)	0	1	3	5	
Form factor	0.67	0.67	0.71	0.73	
NorthWest A319 and A357 Alloys					
Temperature (°C)	563	565	570	574	575
Form factor	0.50	0.53	0.55	0.56	0.57
Soaking time (min)	0	2	3	4	
Form factor	0.61	0.65	0.65	0.69	
Sheffield A357 Alloys					
Temperature (°C)	572	574	576		
Form factor	0.60	0.66	0.70		

The resulting microstructures of the alloys from these experiments were re-examined, and the spheroidicity in terms of form factors was calculated using Eq.[1]. Table II shows the calculated form factors for Alusuisse A356, Northwest A357, Northwest A319, and Sheffield A357 Al alloys under different temperatures and holding times. All the figures validate the results obtained from the load-signal behavior, that

with increasing temperature or holding time, the solid particles become more spheroidal and, hence, the calculated form factor tends toward a value of 1, resulting in lower shear-stress measurements.

An analytical formula following the early work of Dienes and Klemm,[21] derived from the original Stefan's equation for flow between two parallel planes and applied to compression experiments on semisolid Sn15 pct Pb alloy slurries by Laxmanan and Flemings,[19] was used to derive the viscosity of the slug as a function of the average shear rate. Assuming a Newtonian fluid, Laxmanan and Flemings calculated the viscosity of the slug under compression from:

$$F = -\frac{3\eta\nabla^2}{2\pi h^5}\left(\frac{dh}{dt}\right) \qquad [2]$$

where

F = the force which can be obtained from the load-displacement graph,
η = the viscosity,
∇ = the volume of the slug,
h = the instantaneous height of the sample, and
dh/dt = the ram speed.

Strictly, a requirement for the use of this formula to calculate viscosity is that the height, should be much smaller than the slug's diameter; however, it should be noted that this is not met at the beginning of compression carried out in this work and may lead to some initial errors. Assuming that the volume of the sample does not change during compression and that the ram speed remains constant throughout the whole process, the average shear rate can be calculated by integrating throughout the volume:

$$\dot{\gamma}_{avg} = -\frac{R}{2h^2}\frac{dh}{dt} \qquad [3]$$

where R is the instantaneous radius of the sample.

Figures 12 through 14 show the effect of varying the temperatures, holding times, and ram speeds on the viscosity behavior for Alusuisse A356 Al alloys. All the previous figures showed a clear shear-thinning behavior with increasing shear rate. Viscosity values dropped rapidly initially, before gently decreasing to a value with increasing shear rate. Figure 15 shows the viscosity under different temperatures, replotted in a log-log scale. The figure shows a clear pseudo-plastic behavior over the range of shear rates achieved. Values of $n - 1$ vary between -0.99 and -1.31. Given the accuracy of the "curve fit," within experimental error, the viscosity is essentially inversely proportional to the strain rate. The viscosity values dropped by at least half an order of magnitude after the initial breakdown of the skeletal structure in the alloy.

Figure 16 shows the fraction of liquid *vs* temperature for A356 Al alloys, calculated using the commercial software package MTDATA for thermodynamic prediction (from the United Kingdom National Physical Laboratory Teddington, Middlesex). The ternary and binary eutectics are both melting in the temperature region up to 573 °C. The discontinuity

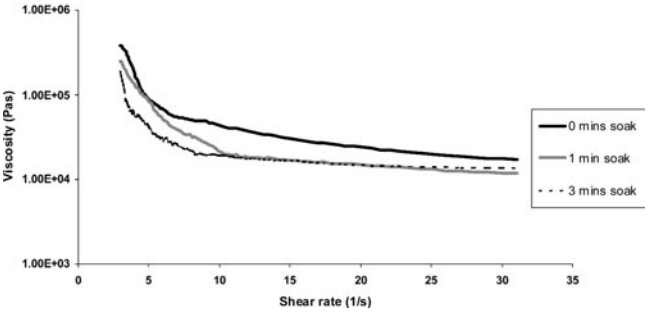

Fig. 13—Effect of soaking times on viscosity under rapid compression of Alusuisse A356 (ram speed: 500 mm/s, T = 575 °C). Average shear rate and viscosity are calculated using the approach of Laxmanan and Flemings.[19]

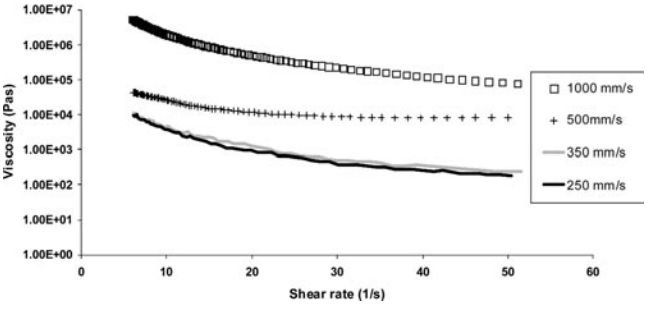

Fig. 14—Effect of different ram speeds on viscosity under rapid compression of Alusuisse A356 Al alloys (0 soak, T = 576 °C). Average shear rate and viscosity are calculated using the approach of Laxmanan and Flemings.[19]

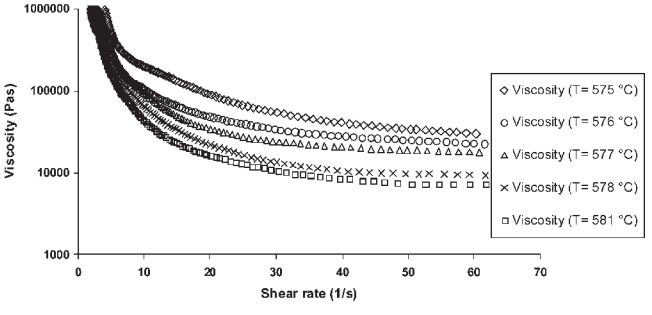

Fig. 12—Effect of temperature on viscosity under rapid compression of Alusuisse A356 Al alloys (ram speed: 500 mm/s, 0 min soak). Average shear rate and viscosity are calculated using the approach of Laxmanan and Flemings.[19]

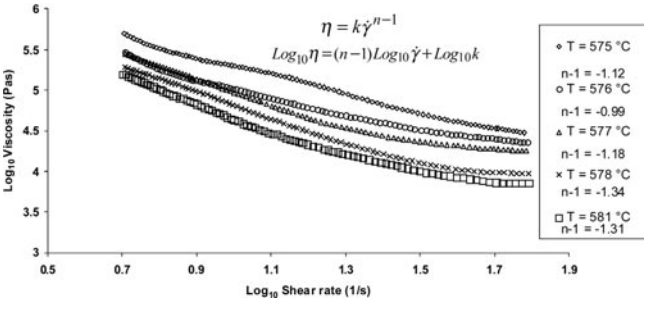

Fig. 15—Calculated viscosity *vs* shear rates based on Laxmanan and Flemings[19] approach replotted in log form for Alusuisse A356 alloys under different temperatures (Fig. 6). The curves are fitted to the power law equation.

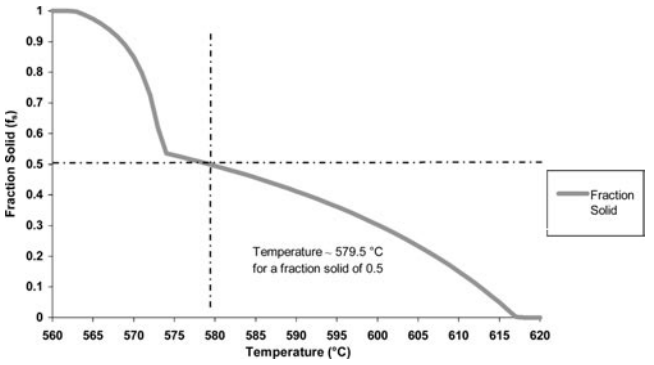

Fig. 16—Fraction solid *vs* temperature for A356 Al alloys (using MT-DATA thermodynamic predictions).

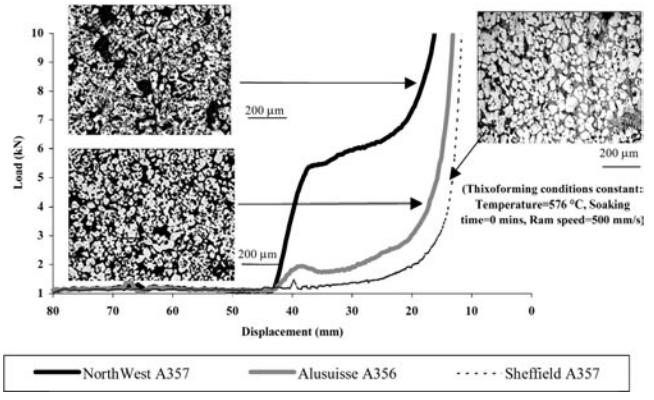

Fig. 17—Load signals and microstructures for different feedstock routes.

at 573 °C marks the end of the eutectic reaction. A further reduction in solid fraction with increasing temperature is associated with the dissolution of the primary Al phase up to the liquidus temperature. Figure 17 compares load signals and microstructures for different feedstock materials. The influence of ram speed on the microstructure in thixoformed discs was examined, comparing the appearance at the edge and the center. At ram speeds of 250 and 350 mm/s, the particles sizes are very similar to each other. However, with increasing ram speed (at 500 and 1000 mm/s), the particles are found to be less spheroidal than those found at the lower speeds when the microstructures at the middle of the samples were examined. Metallographic examination along the edge of the sample showed that the microstructures are similar to each other, regardless of the ram speeds. Figure 18(a) compares the microstructure at the "center" of a thixoformed sample of Alusuisse A356 with that at the "edge."

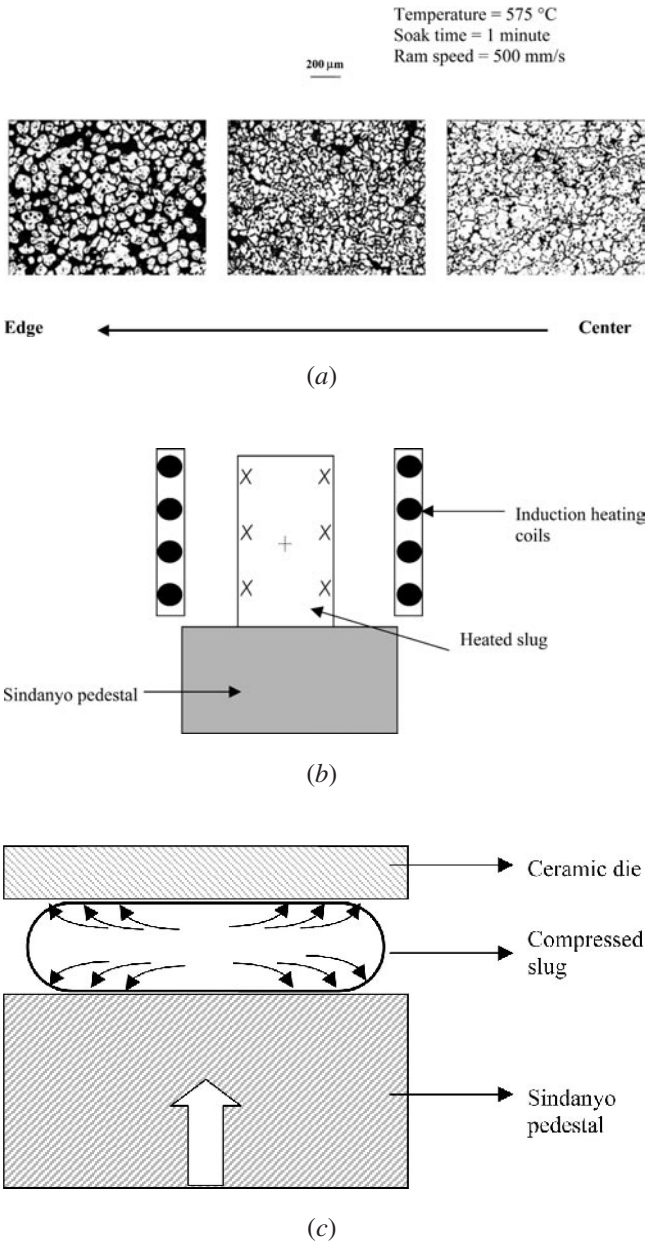

Fig. 18—(*a*) Microstructures of thixoformed sample examined from the "center" to the "edge" (Fig. 3). (*b*) Schematic diagram of the slug during heating. The mechanism of heat generation causes the outer skin of the slug (marked x) to be at a higher temperature at a particular time than the center (marked +). (*c*) Schematic diagram showing the flow field in the slug during thixoforming. The material in the outer skin is subjected to higher shear rate.

IV. DISCUSSION

Figures 9 and 10 reveal the effect of soaking times of up to 5 minutes on the load/displacement plots for Alusuisse A356 at 574 °C and 575 °C for the same ram speed. They demonstrate two points: first, the great sensitivity to temperature, the peak load falling to less than one-half its value with an increase in temperature of 1 °C; and, second, the clear effect of soaking time, where the peak load drops also to one-half its value in 5 minutes of soaking and there is a corresponding fall in the minimum load following the peaks. All these features are significant for industrial thixoforming. One can see from the final microstructures in Figure 9 that the effect of soaking is clearly related to the formation of discrete spheroidized particles from a highly convoluted dendritic morphology in this short period of time. This rapid change in microstructure in a MHD Al/Si alloy during isothermal soaking for short periods in the semisolid state has been previously reported by Loué and Suéry.[23]

The influence of temperature is again shown in Figure 6 for the Alusuisse A356 alloy. These slugs were not soaked

on reaching temperature, but, nevertheless, show a dramatic fall in peak load occurring within the narrow temperature range of 574 °C to 581 °C, corresponding to a decrease in fraction of solid from 0.54 to 0.49. In spite of the relatively small change in temperature (and fraction of solid), the peak has virtually disappeared, and the minimum load at which slurry flow is occurring is about one-tenth of the maximum load at 574 °C and appears to be approximately constant over a range of displacements. Again, these features may be seen as a consequence of morphological changes. The peaks are believed to originate from a three-dimensional skeletal structure built up from the solid phase giving the whole slurry some rigidity, which breaks down under load. The width of the peak (or, more accurately, the downward part of it) is a measure of the time taken to destroy this skeletal structure. A rough estimate of the half-peak width in Figure 6 is 6 mm, which, at a ram velocity of 500 mm/s, gives a breakdown time of 12 ms: this is one order of magnitude shorter than the relaxation times obtained from shear-rate jumps in rotational viscometer experiments[24,25,26] and is clearly related to a different mechanism. The height of the peak falls with temperature as the skeletal structure is consumed, and the minimum load beyond the peak also decreases with increasing temperature, both because a more spheroidal particle morphology is developed and the fraction of liquid increases. This effect may be interpreted simply in terms of the increase in average distance between particles (or clusters of particles), since if the bulk of the shearing takes place within the liquid phase, an increase in the average distance will result in a lower shear rate and, therefore, will lower both the shear stress and apparent viscosity.

The results of Figure 6 have been replotted in Figure 15 on a log/log scale. If the viscosity can be represented as a power law of the form

$$\eta = \kappa \dot{\gamma}^{n-1} \quad [4]$$

then the plot should be linear with a slope of $(n - 1)$. Figure 15 reveals that this is approximately true for all the temperatures over the narrow range of shear rates, showing shear thinning with a slope of around -1, in agreement with earlier investigations.[20,27] There is no doubt that the viscosity is highly dependent on the temperature (or fraction of solid) of testing over the whole range of shearing rates.

The effect of ram speed is illustrated in Figure 11 and reproduced as viscosity as a function of average shear rate in Figure 14. It is clear that not only is the alloy slurry pseudoplastic, showing shear-thinning behavior, it is also thixotropic in that it is time dependent. At a given shear rate, the viscosity increases with increasing ram velocity: that is, with a shorter time to achieve the same shear rate. These measured viscosities are also much higher than those measured in steady-state experiments.[24] We cannot, therefore, use steady-state viscosities to describe flow during industrial thixoforming: this conclusion is contrary to that expressed by Yurko and Flemings.[27] At ram speeds of 250 and 350 mm/s, the particle sizes are very similar to each other. However, with increasing ram speed (at 500 and 1000 mm/s), the particles are found to be less spheroidal than those found at the lower speeds when the microstructures at the middle of the samples were examined. The more-spheroidal particles at the lower speed seem to correspond to the lower-force load signals obtained in Figure 11. This effect could be attributed to more spheroidal particles being forced toward the edge of the die with increasing ram speed. Metallographic examination along the edge of the sample showed that the microstructures are similar to each other regardless of the ram speeds. Figure 18(a) shows the microstructures taken from the center to the edge of the sample after thixoforming. Clearly, the particles are more spheroidal toward the edge than at the center. This may be due to the generation of heat in the outer skin of the slug during induction heating to the semisolid state. The outer edge of the slug (Figure 18(b), marked "*x*") will experience a higher temperature for a longer time than the center of the slug as the heat is generated. As a result, more liquid and spheroidal particles will be formed and, upon compression, this material will be at the outer edge in the thixoformed disc. In addition, on compression, it is assumed that the flow field is such that the outer edge will be subjected to higher shear (Figure 18(c)).

Finally, we consider the effect of the different processing routes and alloys given in Figure 6 (Alusuisse A356), Figure 7 (Northwestern A319), and Figure 8 (Sheffield A357). Direct comparisons are difficult to make, since compositional differences will produce different fractions of solid at the same temperature. However, in each case, the peak and the flow load drop significantly with increased temperature. The peak width is noticeably narrower in the Sheffield alloy, indicating a shorter skeletal breakdown time (~8 ms), whereas a broader peak appears in the Northwestern alloy, indicating a longer time (~14 ms). The load levels exhibited by these three alloys probably reflect their microstructural differences. The Sheffield alloy clearly develops a very spheroidized microstructure as the temperature is increased to 576 °C (FF = 0.70) compared to the Alusuisse alloy (FF = 0.64), whereas the Northwestern alloy still retains a complex and intricate microstructure containing entrapped liquid within the solid, even at the highest test temperature (FF = 0.57). It is the nonspheroidized structures that can form the most stable and rigid skeletal structures, having a multiplicity of particle contacts while preserving larger clusters even when the skeleton has been destroyed. This will contribute both to higher peaks initially and to higher stresses and viscosities during subsequent flow (Figure 17). Loué and Suéry[23] have measured the spheroidization in a semisolid A17 pct Si MHD alloy during isothermal soaking over very long periods of time, and Tzimas and Zavaliangos[28] have performed similar experiments on the same alloy with up to 5 minutes of soaking. Both researchers record rapid spheroidization of the initial dendritic structure within the first few minutes, and Loué and Suéry demonstrate that this continues for at least 30 minutes. This is clear support for the observations in the present work and the consequences on the flow behavior. Tzimas and Zavalinagos[28] observed that the inhomogeneous microstructure in an as-produced MHD alloy would result in agglomeration of solid with liquid pools between the liquid and solid phases. A similar effect was seen by these workers using a SIMA or RAP starting material, in which the slurry is initially nondendritic; however, the spheroidization process is not so evident. These observations seemed to correspond to the results obtained in this work (*i.e.*, the lower load detected for the Sheffield

RAP alloys compared to the MHD Alusuisse alloys (*c.f.* Figure 17)).

Comparison of the presently calculated viscosities with previous work on A1-Si alloys is presented in Figure 19. It is important to be aware that small changes in silicon content can affect the results quite considerably by changing the fraction of solid.[20,23] Comparing the viscosity at 578 °C of the Alusuisse A356 alloy used in this work (which contains 6.6 pct Si), it is slightly higher than that found by Loué *et al.*[20] for A356 (nominally containing 6 pct Si) at 580 °C. However, in the work by Loué *et al.*, their alloy was soaked isothermally for 30 minutes before undergoing deformation by backextrusion, whereas our values are derived from slugs having no soaking at the test temperature. This is most probably the explanation of the discrepancy, given our knowledge of the effect of soaking on microstructure and viscosity. The lower values recorded by Yurko and Flemings[27] are derived from alloy containing a higher silicon content which was also soaked for 30 minutes before testing. Both these factors will give rise to the reduction of viscosity observed in Figure 19. Included in this figure is the steady-state viscosity determined by Quaak[24] for a 7 pct Si aluminum alloy, extrapolated to a 0.5 fraction of solid: this is well below the other determinations using relatively short-time experiments, emphasizing the fact that steady state is not achieved in the latter, nor in industrial thixoforming.

Extrapolation of the results of Loué *et al.*[20] and Yurko and Flemings[27] to very low strain rates (less than 10^{-4} s^{-1}) indicates that viscosities in excess of 10^7 Pa.s may be achieved. A simple calculation, based on an example by Flemings[3] of the slumping by 1 mm of a billet (50-mm high) under its own weight at this viscosity, suggests that it would take several minutes for this change in height to be achieved. For all practical purposes, this is unimportant.

V. CONCLUSIONS

Rapid-compression experiments have provided a method to assess the thixoformability of various aluminum feedstock alloys. By relating their microstructures (including the effect of liquid content) with the load signal encountered, several insights have been gained into the effect of different thixoforming conditions. They are as follows.

1. The load-displacement plots of semisolid alloys characteristically exhibit an initial peak which falls to a minimum load when the slurry begins to flow. The peak load has been associated with a skeletal structure resisting flow, which rapidly breaks down under shear (in ~10 ms) to generate a shear-thinning slurry.
2. The peak load and flow load both fall with increasing soaking time at isothermal temperature for up to 5 minutes in the Alusuisse A356 alloy, as a consequence of microstructural changes which produce more spheroidized and discrete solid particles within the liquid matrix. Increasing the soaking temperature also causes the disappearance of the peak and results in easier flow, both from microstructural changes and from an increase in the fraction of liquid.
3. Analysis of the load-displacement plots provides information on the viscosity–shear-rate behavior, which clearly demonstrates shear thinning at all temperatures in this alloy, with a power-law index of ~−1. Experiments using different ram velocities show that the viscosity is time dependent (*i.e.*, thixotropic) for a given shear rate, and

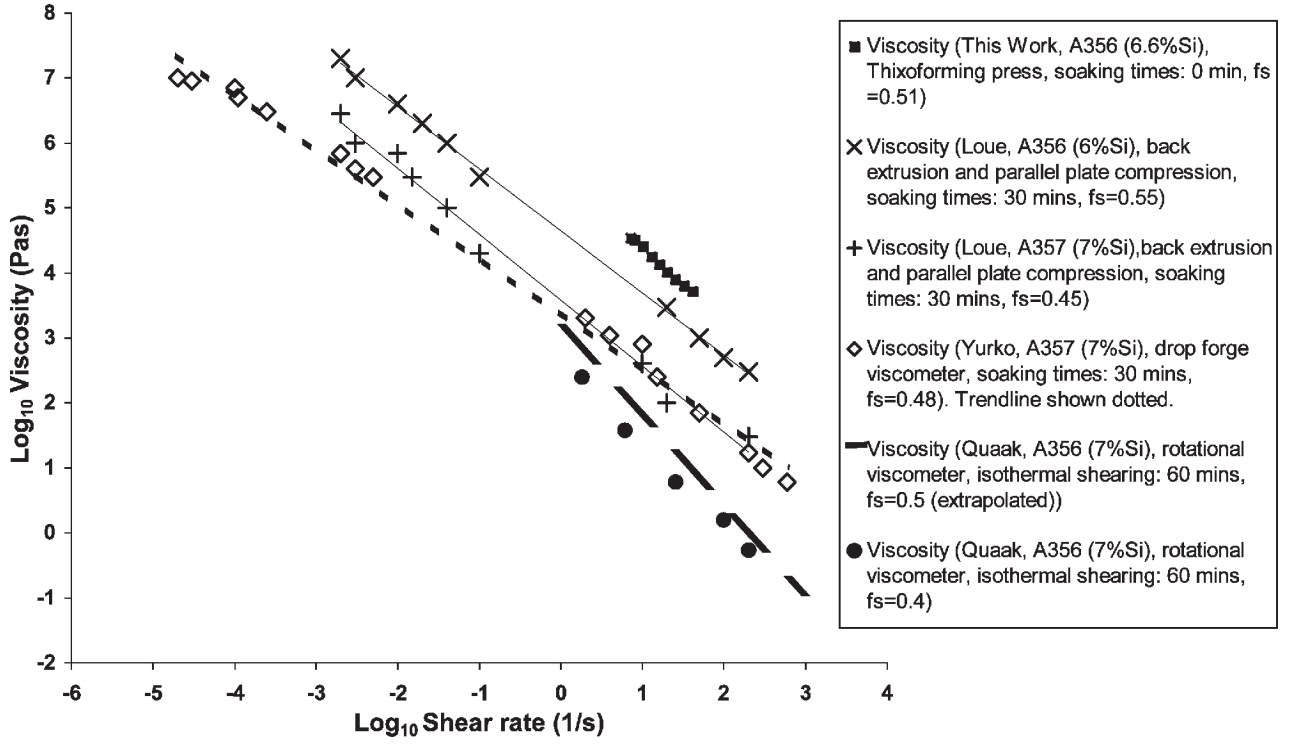

Fig. 19—Comparison of apparent viscosities obtained by various experimental techniques and conditions.

that steady-state viscosity values are not pertinent to real industrial thixoforming conditions.

4. Comparison of the Alusuisse A356 alloy with previous work on similar aluminum alloys shows that the present alloy possesses a higher viscosity in the narrow range of shear rates investigated, although with an equivalent power-law index. This is attributed to the long soaking times (~30 minutes) used in the previous work.
5. Work on aluminum alloys having different compositions and production routes shows similar characteristics to the Alusuisse A356; that is, increased soaking times and temperatures reduce peak loads and flow loads as the microstructure becomes more spheroidized.

ACKNOWLEDGMENTS

The authors thank Dr P.J. Ward for his most helpful discussions. This work was carried out as part of EPSRC Grant No. GR/L/98473.

REFERENCES

1. D.B. Spencer, R. Mehrabian, and M.C. Flemings: *Metall. Trans.*, 1972, vol. 3, pp. 1925-32.
2. P.A. Joly and R. Mehrabian: *J. Mater. Sci.*, 1976, vol. 11, pp. 1393-418.
3. M.C. Flemings: *Metall. Trans. A*, 1991, vol. 22A, pp. 957-79.
4. D.H. Kirkwood: *Int. Mater. Rev.*, 1994, vol. 39, pp. 173-89.
5. M.P. Kenney, J.A. Courtois, R.D. Evans, G.M. Farrior, C.P. Kyonka, A.A. Koch, and K.P. Young: *Metals Handbook*, 9th ed., ASM INTERNATIONAL, Metals Park, OH, 1988, vol. 15, pp. 327-38.
6. J.P. Gabathuler, H.J. Huber, and J. Erling: *Proc. Int. Conf. on "Aluminium Alloys: New Process Technologies*", Ravenna, Italy, 1993 Publ., Associazione Italiana di Metallurgia, Milan, pp. 169-80.
7. K.P. Young, C.P. Kyonka, and J.A. Courtois: U.S. Patent 4-415-374, 1983.
8. D.H. Kirkwood, C.M. Sellars, and L.G.E. Boyed: U.S. Patent 5-133-811, 28/07/1992.
9. S.C. Bergsma, M.C. Tolle, E. Evangelista, M.E. Kassner, and X. Li: *Proc. 5th Int. Conf. on "Semisolid Processing of Alloys and Composites,"* Golden, CO, 1998, A.K. Bhasin, J.J. Moore, K.P. Young, and S. Midson, eds. Colorado School of Mines, Golden, CO, 1998, pp. 149-55.
10. A. Leatham, A. Ogilvy, P. Chesney, and J.V. Wood: *Metall. Mater.*, 1989, vol. 5 (3), pp. 140-43.
11. M. Kiuchi and S. Sugiyama: *Proc. 2nd Int. Conf. on "Semisolid Processing of Alloys and Composites,"* Cambridge, MA, 1992, S.B. Brown and M.C. Flemings, eds. Massachusetts Institute of Technology Press, Cambridge, MA, 1992, pp. 47-56.
12. T. Haga and S. Suzuki: *Proc. 6th Int. Conf. on Semisolid Processing of Alloys and Composites*, Turin, Italy, 2000, G.L. Chiarmetta and M. Rosso, eds., Edimet Spa, Brescia, Italy, 2000, pp. 735-40.
13. European Patent Specification FP 0-745-694-A1, UBE Industries Ltd., Japan.
14. K. Hall, H. Kaufmann, and A. Mundl: *Proc. 6th Int. Conf. on Semisolid Processing of Alloys and Composites*, Turin, Italy, 2000, G.L. Chiarmetta and M. Rosso, eds. Edimet Spa, Brescia, Italy, 2000, pp. 23-28.
15. P. Kapranos: *Proc. 4th Int. Conf. on Semisolid Processing of Alloys and Composites*, Sheffield, United Kingdom, 1996, D.H. Kirkwood and P. Kapranos, eds. University of Sheffield, Sheffield, UK, 1996, pp. 360-62.
16. D.H. Kirkwood and P. Kapranos: *Met. Mater.*, 1989, vol. 5, pp. 16-19.
17. P. Kapranos, D.H. Kirkwood, and M.R. Barhudarov: *Proc. 5th Int. Conf. on Semisolid Processing of Alloys and Composites*, Golden, CO, 1998, A.K. Bhasin, J.J. Moore, K.P. Young, and S. Midson, eds. Colorado School of Mines, Golden, CO, 1998, pp. 11-19.
18. P. Kapranos, T.Y. Liu, H.V. Atkinson, and D.H. Kirkwood: *J. Mater. Processing Technol.*, 2001, vol. 111, pp. 31-36.
19. V. Laxmanan and M.C. Flemings: *Metall. Trans. A*, 1980, vol. 11A, pp. 1927-36.
20. W.R. Loué, M. Suéry, and J.L. Querbes: *Proc. 2nd Int. Conf. on Semisolid Processing of Alloys and Composites*, Cambridge, MA 1992, S.B. Brown and M.C. Flemings, eds., Massachusetts, pp. 266-75.
21. G.J. Dienes and H.F. Klemm: *J. Appl. Phys.*, 1946, vol. 17, pp. 485-511.
22. T. Witulski, U. Morjan, I. Niedick, and G. Hirt: *Proc. 5th Int. Conf. on Semisolid Processing of Alloys and Composites*, Golden, CO, 1998, A.K. Bhasin, J.J. Moore, K.P. Young, and S. Midson, eds., Colorado School of Mines, Golden, CO, 1998, pp. 353-60.
23. W.R. Loué and M. Suéry: *Mater. Sci. Eng. A*, 1995, vol. 203, pp. 1-13.
24. C.J. Quaak: Ph.D. Thesis, Technische Univesiteit Delft, Delft, The Netherlands, 1996.
25. T.Y. Liu, P.J. Ward, D.H. Kirkwood, and H.V. Atkinson: *XIIIth Int. Congr. on Rheology*, Cambridge, United Kingdom, 2000, D.M. Binding, N.E. Hudson, J. Mewis, J.-M. Piau, C.J.S. Petrie, P. Townsend, M.H. Wagner, and K. Walters, eds., British Society of Rheology, Glasgow, United Kingdom, 2000, vol. 4, pp. 61-63.
26. T.Y. Liu, H.V. Atkinson, P.J. Ward, and D.H. Kirkwood: *Metall. Mater. Trans. A*, 2003, vol. 34A, pp. 409-17.
27. J.A. Yurko and M.C. Flemings: *Metall. Mater. Trans. A*, 2002, vol. 33A, pp. 2737-46.
28. E. Tzimas and A. Zavaliangos: *J. Mater. Sci.*, 2000, vol. 35, pp. 5319-29.